ORTHODONTICS & CRANIOFACIAL RESEARCH

ORIGINAL ARTICLE

T Yoshida
M Yamaguchi
T Utsunomiya
M Kato
Y Arai
T Kaneda
H Yamamoto
K Kasai

Low-energy laser irradiation accelerates the velocity of tooth movement via stimulation of the alveolar bone remodeling

Authors' affiliations:
T. Yoshida, M. Yamaguchi, K. Kasai, Department of Orthodontics, Nihon University School of Dentistry at Matsudo, Chiba, Japan
T. Utsunomiya, H. Yamamoto, Department of Oral Pathology, Nihon University School of Dentistry at Matsudo, Chiba, Japan
M. Kato, T. Kaneda, Department of Radiology, Nihon University School of Dentistry at Matsudo, Chiba, Japan
Y. Arai, Nihon University School of Dentistry, Tokyo, Japan

Correspondence to:
Takamasa Yoshida or *Masaru Yamaguchi*
Department of Orthodontics
Nihon University School of Dentistry at Matsudo
2-870-1 Sakaecho-Nishi
Matsudo, 271-8587 Chiba
Japan
E-mail: yoshida.takamasa@nihon-u.ac.jp, yamaguchi.masaru@nihon-u.ac.jp

Dates:
Accepted 7 January 2009

To cite this article:
Yoshida T, Yamaguchi M, Utsunomiya T, Kato M, Arai Y, Kaneda T, Yamamoto H, Kasai K: Low-energy laser irradiation accelerates the velocity of tooth movement via stimulation of the alveolar bone remodeling
Orthod Craniofac Res 2009;**12**:289–298

Structured Abstract

Authors – Yoshida T, Yamaguchi M, Utsunomiya T, Kato M, Arai Y, Kaneda T, Yamamoto H, Kasai K

Introduction – Previously, the authors have reported the acceleration of tooth movement and osteoclastogenesis on the pressure site in an experimental tooth movement model by low-energy laser irradiation (LELI), which stimulated the RANK/RANKL system and *c-fms*/macrophage colony-stimulating factor system. However, the effect of LELI on osteogenesis on the tension site is not known clearly. Moreover, the temporal changes in alveolar bone during tooth movement have not been investigated as yet. Therefore, the present study was designed to examine the effects of LELI on alveolar bone remodeling during experimental tooth movement, and observe the temporal bone mineral density (BMD) using micro-computed tomography (μCT).

Materials and methods – To induce experimental tooth movement in rats, 10 g force was applied to the upper right first molar with Nickel titanium closed-coil. Next, a gallium-aluminum-arsenide (Ga-Al-As) diode laser was used to irradiate the area around the moved tooth, and BMD and the amount of tooth movement were measured by μCT scanning for 21 days. Histopathological examination was also performed.

Results – The amount of tooth movement in the LELI group was significantly greater than in the non-irradiation group by the end of the experimental period. Further, compared with the non-irradiation group, the fall of BMD was less in the LELI group.

Conclusion – These findings suggest that LELI accelerates the velocity of tooth movement via stimulation of the alveolar bone remodeling.

Key words: bone mineral density; experimental animal model; Laser therapy, low level; tooth movement; X-Ray microtomography

Introduction

Orthodontic treatment is useful to achieve an optimal dental arch form for each patient, and create a smooth functional occlusion by tooth movement. However, since the treatment period is very long and a great burden for the patient, shortening of the duration is desired. When orthodontic

force is applied to a tooth, osteoclastogenesis occurs on the pressure site, and osteogenesis occurs on the tension site. These stimulate alveolar bone remodeling surrounding the root, and the tooth moves (1–3). In physiological remodeling, the amount of bone resorption and formation are almost equal, and bone mass does not change after remodeling (4). This is called coupling of bone resorption and formation, and bone remodeling is materialized by this coupling balance. Therefore, in remodeling caused by orthodontic force, it is likely that the coupling balance shifts to bone resorption on the pressure site, and bone formation on the tension site. Tooth movement causes remodeling in a limited part of the alveolar bone, and the coupling mechanism during such remodeling is still unknown.

Yamaguchi et al. (5) and Fujita et al. (6) reported that low-energy laser irradiation (LELI) accelerated tooth movement and osteoclastogenesis on the pressure site via stimulation of the receptor activator of nuclear factor-*k*B (RANK)/RANK ligand (RANKL) system and the *c-fms*/macrophage colony-stimulating factor system during experimental tooth movement. These reports suggest that LELI accelerates bone remodeling, thus shortening the orthodontic treatment period. However, little is known about the effect of LELI during alveolar bone remodeling on the tension site *in vivo*, although Kawasaki et al. (7) reported that LELI increases bone area.

Conventionally, a thin section of bone is prepared and observed under the microscope to examine the structure of bone (8–10), and skill is required for preparation, pretreatment, such as embedment, and measurement. Recently, micro-computed tomography (μCT) was introduced as one of the various bone mass measuring methods (11–15), and applied for detailed observation of bone structure (16–18). This required neither difficult pretreatment of the specimen nor technical skill, and non-invasive measurement was possible (19). Therefore, μCT may also be applied in dentistry for various research examinations (20, 21). Furthermore, the advent of the *in vivo* μCT (R_mCT®; Rigaku, Tokyo, Japan) (22) enabled us to observe temporal changes, without sacrificing the same sample. There are still few reports which observed temporal changes of alveolar bone under tooth movement in the same sample. Moreover, in order to understand the process of osteogenesis, combined use of histopathological observation and X-ray photography is effective (23). Therefore, the present study was designed to examine the effects of LELI on alveolar bone remodeling during experimental tooth movement, and observe the temporal bone mineral density (BMD) using μCT and histopathological observation.

Materials and methods

Experimental animals

A total of 60 male Wistar strain rats (Sankyo Labo Service Co, Tokyo, Japan) aged 6 weeks old (180 ± 10 g) were used for the experiments. They were kept in separate cages at the Animal Center of Nihon University School of Dentistry at Matsudo, with a 12-h light/dark environment at a constant temperature of 23°C, and provided with food and water *ad libitum*. The health status of each rat was evaluated by daily monitoring the body weight for 1 week before the start of the experiments.

Experimental tooth movement

Sixty rats were divided into two groups of 30 rats each, to form the LELI, and non-irradiation groups. All operations were carried out under general anesthesia by administering an intraperitoneal injection of Pentobarbital sodium (40 mg/kg). Experimental tooth movement was performed using the method of Fujita et al. (6), in which a Nickel titanium closed-coil spring (NT-coil) (wire diameter, 0.15 mm; outer coil diameter, 1.10 mm; Furukawa Techno Material Co., Kanagawa, Japan) was ligated to the maxillary right first molar using stainless steel ligature wire (wire size: 0.20 mm, Tomy International Inc., Tokyo, Japan). The other end of the NT-coil was also ligated to holes in the maxillary incisors drilled laterally just above the gingival papilla with a No. 1/4 round bar, using the same ligature wire. The upper right first molar was moved mesially using NT-coil with 10 g force (Fig. 1). The force was determined based on previous reports (24, 25) which showed that the rat upper first molar could be moved by light continuous force without a decrease in body weight or creating hyalinized degenerative tissues. The experiments were performed for a period of 22 days (day 0–21) (Fig. 2). The animal experimental protocol in the present study was approved by the Ethics Committee for Animal Experiments of our university (approval No. ECA-08-0001).

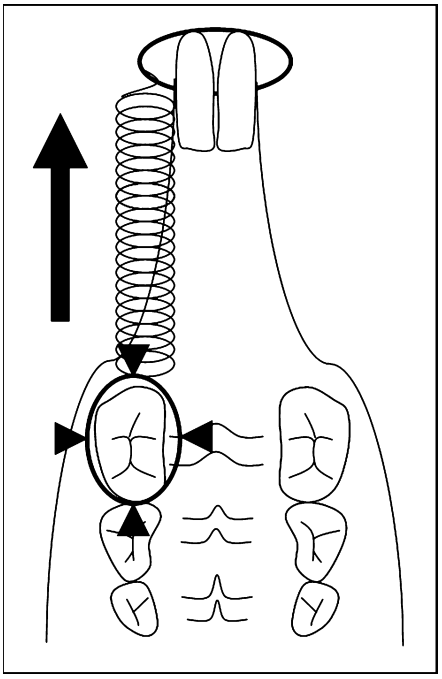

Fig. 1. Experimental tooth movement appliance and LELI points. The upper right first molar was moved mesially by NT-coil spring at 10 g force. Arrow, force direction; arrow heads, LELI points.

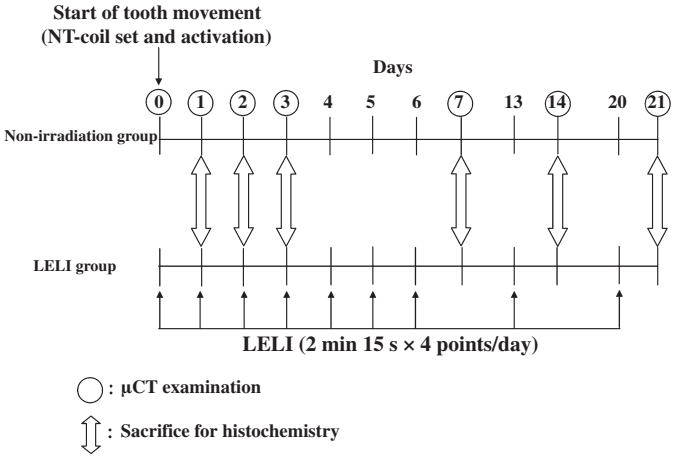

Fig. 2. Experiment time-schedule for each group.

Laser irradiation

A gallium-aluminum-arsenide (Ga-Al-As) diode laser (Osada Inc., Tokyo, Japan) with wavelength 810 nm forming continuous waves at 100 mW output power condition was used. These irradiation conditions were based on the method of Fujita et al. (6) The laser beam was delivered by a 0.6-mm-diameter optical fiber, and irradiation was administered, under anesthesia, by placing the end of the optical fiber tip in contact with the mesial, distal, buccal, and palatal sides of the gingiva in the area of the upper right first molar to be moved (Fig. 1). Irradiation was performed for 2 min and 15 s at each point (total 9-min) once daily on days 0–6, days 13, and days 20 (total nine times) (Fig. 2). Total energy corresponding to a 9-min exposure was 54.0 J/cm^2, which was similar to the dose used by Fujita et al. (6) In addition, the LELI group was given general anesthesia during these procedures to less the burden on the rats. The non-irradiation group served as control.

Scanning parameters of μCT

The authors used *in vivo* μCT at a magnification of 6.7 fold (voxel size: 30 × 30 × 30 μm), tube voltage of 75 kv, and tube current of 80 μA. The image reconstruction software used was i-view-R (J. Morita mfg. corp., Kyoto, Japan). The field of view was 14.4 × 14.4 × 14.4 mm (pixel number: 480 × 480 × 480), and scanning time was 17 s. μCT examination was performed once a day on days 0–3, day 7, day 14, and day 21 (total seven times) (Fig. 2).

Measurement of tooth movement and BMD

Determination of the amount of tooth movement and the analysis of measurement μCT examination data of BMD were performed with BMD Measuring Software (Kitasenjyu Radist Dental Clinic, i-view Image Center, Tokyo, Japan). BMD measuring area of this software extended from the distal side of the distobuccal root, and was made into the shape of a rectangular parallelepiped (600 × 480 × 1500 μm) containing the periodontal ligament (PDL) of the distobuccal root (Fig. 3BMD, PDL). The rectangular parallelepiped was 600 μm in buccopalatal width according to the width of the distobuccal root, set it up with 480 μm in mesiodistal width because avoided interference of the mesiobuccal root of second molar with a measuring area, and set up height with 1500 μm according to length of the distobuccal root (Fig. 3X, Y, Z and BMD).

In this software, the position of the rectangular parallelepiped, which was a measuring area, was checked by three tomograms, X plane, Y plane, and Z plane (Fig. 3X, Y and Z). Two solid lines which showed the measuring range were displayed on each plane (Fig. 3 red lines, green lines and blue lines). Moreover, the dashed line inserted into two solid lines corresponded to the center of the measuring range, and showed the position of each tomogram (Fig. 3X, Y and Z). The line

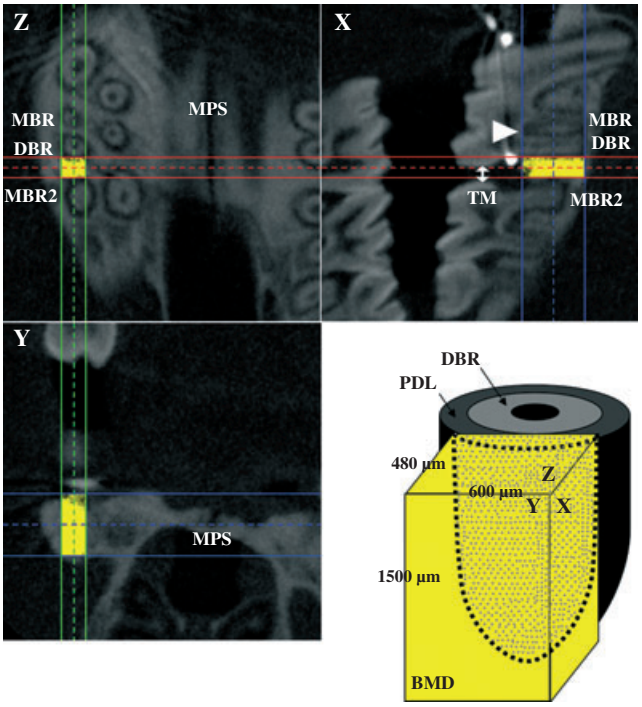

Fig. 3. Setting of the tooth position and BMD measurement area. X, X plane; Y, Y plane; Z, Z plane; BMD, measurement area for BMD, TM (bidirectional arrow): measurement area for tooth movement; Green lines, X plane is shown; Red lines, Y plane is shown; Blue lines, Z plane is shown, MBR, mesiobuccal root of first molar; DBR, distobuccal root of first molar; MBR2, mesiobuccal root of second molar, MPS, mid palatal suture; arrow head, root furcation of DBR and MBR; PDL, periodontal ligament; Dots, PDL contained in measurement area.

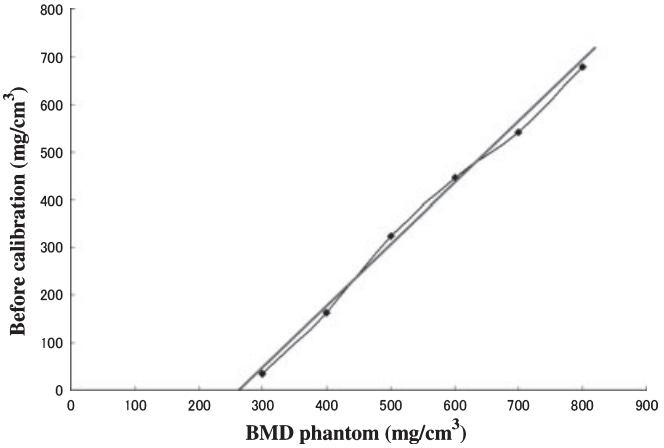

Fig. 4. Calibration curve of BMD. Multiple correlation coefficient: $R = 0.998$, Regression equation: $y = 1.28x - 339.74$.

that showed the measuring range was rotated or moved parallel, and position of the rectangular parallelepiped was set up. Actually in X plane, a solid line by the mesial side of the red lines and the distal side of distobuccal root coincided (Fig. 3X red lines and DBR), and a solid line by the coronal side of blue lines which intersected perpendicularly with the red lines coincided with the height of the root furcation of distobuccal root and mesiobuccal root (Fig. 3X DBR, MBR and arrow head). In Y plane, the green lines and the tooth axis of distobuccal root coincided (Fig. 3Y, green lines). In Z plane, the green lines and the mid palatal suture (MPS) coincided. A parallel translation of it was carried out and it was made to coincide with the center of the distobuccal root (Fig. 3Z green lines, MPS and DBR).

These operations determined the position of the experimentally moved tooth and the distance between contacts of the mesiobuccal root of the second molar was measured with the distance measurement tool of this software as the amount of tooth movement (Fig. 3X, bidirectional arrow). BMD was calculated from the bone mineral content of the above-mentioned rectangular parallelepiped, and it was divided by the rectangular parallelepiped volume. Therefore, the calculated BMD showed average BMD of the area containing the PDL of the distal side of distobuccal root (Fig. 3 BMD, PDL). In addition, BMD was calibrated the BMD phantom of 300, 400, 500, 600, 700, and 800 mg/cm^3 (Fig. 4).

Tissue preparation

The experimental periods for observation were set at 1, 2, 3, 7, 14 and 21 days after tooth movement. Each group of rats was further divided into day 0–1, day 0–2, day 0–3, day 0–7, day 0–14 and day 0–21 subgroups, with five rats in each. Each rat was deeply anesthetized and perfused with 10% formalin solution in 0.1 M phosphate buffer solution in a trans-cardial manner, after which the maxilla was immediately dissected and immersed in the same fixative overnight at 4°C. The specimens were decalcified in a 10% disodium ethylenediamine tetracetic acid (EDTA, pH 7.4) solution for 4 weeks, and the decalcified specimens were dehydrated through an ethanol series and embedded in paraffin in usual method. Each sample was sliced into 4 μm serial sections in the horizontal direction, and stained with hematoxylin and eosin (HE).

Histopathological observation

The HE-stained sections were observed under an optical microscope. The part corresponding to the Z

plane image was chosen as the observation area for μCT (Figs 3Z and 5). The PDL and alveolar bone on the tension site between the distal side of distobuccal root of the experimentally moved tooth, and the mesial side of mesiobuccal root of the second molar were observed (Fig. 5 DBR, MBR2 and TS).

Statistical analysis

BMD was calibrated measurement of the BMD phantom by regression analysis. The values shown represent the mean ± SD for each group. Intergroup comparisons of the average values were performed with Mann–Whitney *U*-test for body weight, amount of tooth movement, and BMD. A value of $p < 0.05$ was considered to indicate a significant difference.

Results

Tooth movement during the experimental period

The body weights of the rats in the LELI and non-irradiation groups showed an increase with time. No significant differences were found between the two groups. A space was detected between the first and second molars because the first molar was moved mesially (Fig. 6 arrows). In contrast, there was no space between the second and third molars (Fig. 6 arrow heads). The amount of tooth movement was significantly greater in the LELI group on days 3 (1.4-fold), 7 (1.19-fold), 14 (1.26-fold), and 21 (1.34-fold) than in the non-irradiation group (Fig. 7).

HE and μCT image findings

One day after the start of tooth movement (Fig. 8A, 1 day), expansion of the PDL fibers which followed the direction of tooth movement, and extension of the blood vessels were detected in both groups of the LELI and the non-irradiation (Fig. 8A, L6, N6, BL6a and N6-f). Moreover, a few multinucleated giant cells corresponding to osteoclasts were partly observed on the alveolar bone surface of the tension sites of both groups. Further, an increase in the number of osteoclasts was recognized in both groups on days 2 (data not presented) or 3, and this tendency was strongly seen in the LELI group (Fig. 8A, L7, N7, B, L7-b and N7-g). On day 7, in both groups, the number of osteoclasts decreased, dilatation of the blood vessels and proliferation of the fibroblasts in the PDL increased, and polygonal osteoblast cells were increasingly identified on the alveolar bone surface (Fig. 8A, L8, N8, B, L8-c and N8-h). On day 14, trabecular bone formation

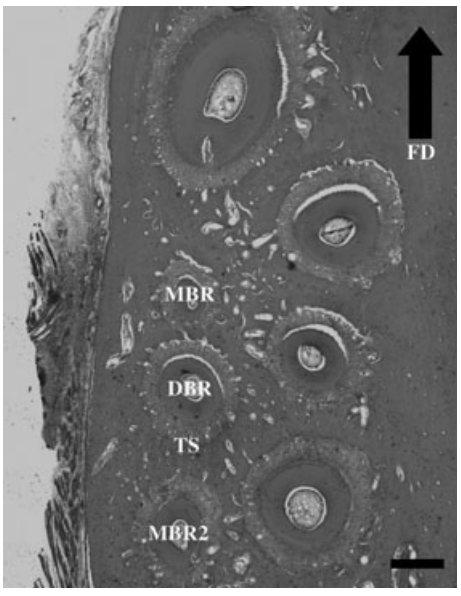

Fig. 5. Observation area in the optical microscope (×20, Bar: 500 μm). MBR, mesiobuccal root of first molar; DBR, distobuccal root of first molar; MBR2, mesiobuccal root of second molar; TS, tension site; arrow FD, force direction.

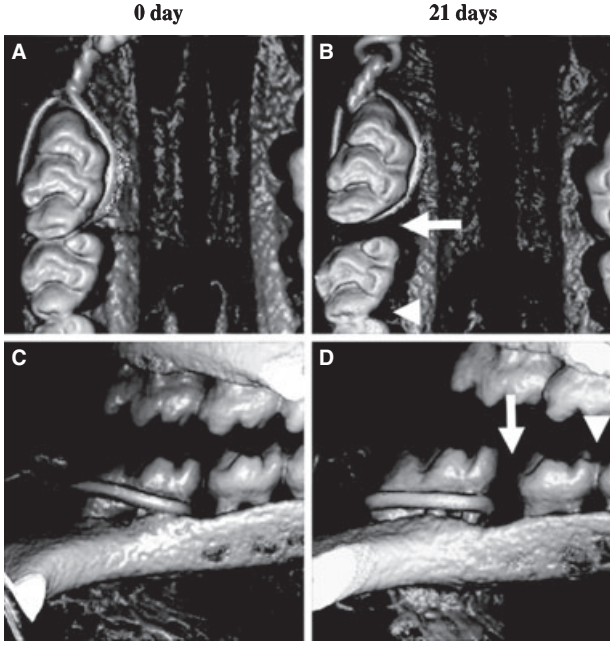

Fig. 6. Tooth movement system in rat. Distinct movement space (arrows) was detected between the first and second molars at days 0 (A, C) and 21 (B, D). In contrast, there was no space between the second and third molars (arrow heads).

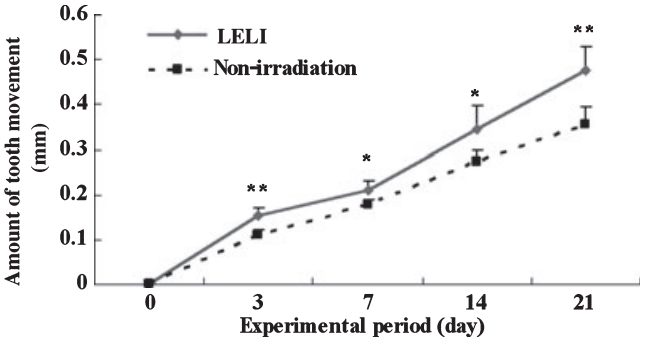

Fig. 7. Amount of tooth movement. It was significantly greater in the LELI group than in the non-irradiation group (**$p < 0.01$, *$p < 0.05$, N = 5).

on the tension site was noted in both groups, and this tendency was strong in the LELI group (Fig. 8A, L9, N9, B, L9-d and N9-i). On day 21, there was alveolar bone resorption with increase in the amount of tooth movement in both groups, and this tendency was strong in the non-irradiation group (Fig. 8A, L10, N10, B, L10-e and N10-j). In addition, the width of the PDL space after 1 day was not further reduced throughout the experimental period as confirmed by the temporal μCT image of the same sample (Fig. 9, L1-5 and N1-5), and comparison with HE and μCT images (Fig. 8A, L1-10 and N1-10).

BMD

The multiple correlation coefficient was $R = 0.998$ as the regression analysis. The obtained regression equation was

$$y = 1.28x + 339.74$$

calibrated BMD using this formula (Fig. 4). Both groups showed a temporal fall in BMD with increase in the amount of tooth movement. BMD was significantly greater in the LELI group on days 7 (1.08-fold), 14 (1.09-fold), and 21 (1.14-fold) than in the non-irradiation group (Fig. 10).

Discussion

Several studies of the amount of tooth movement after LELI have been reported. Fujita et al.(6) indicated that

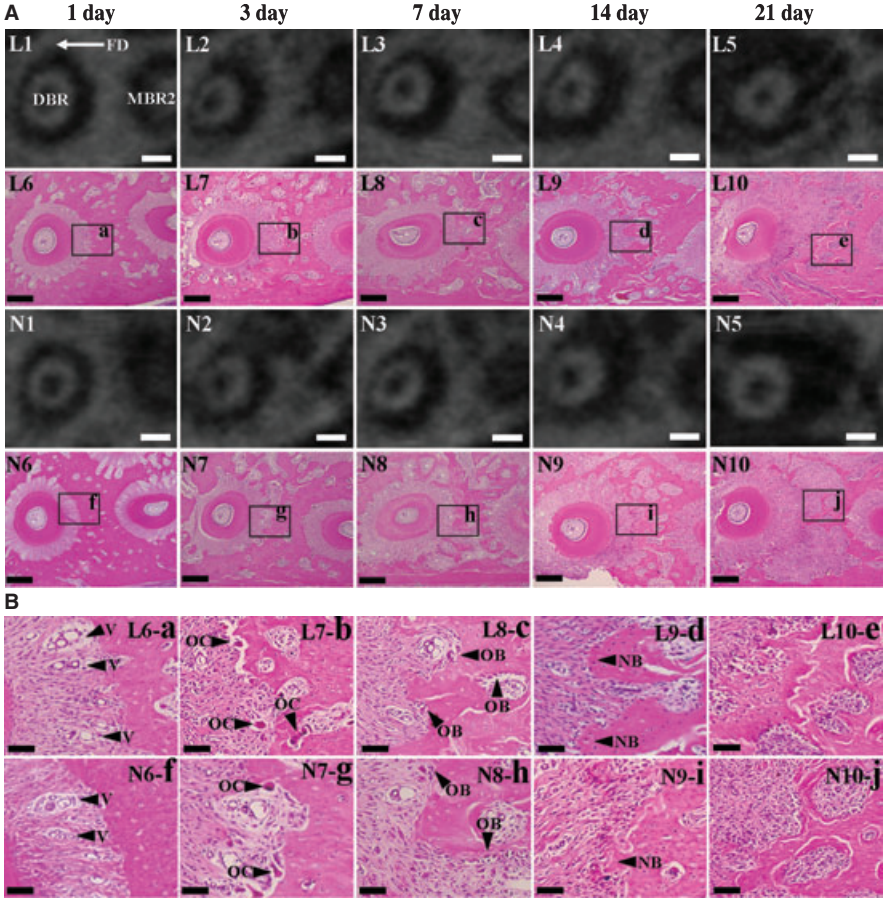

Fig. 8. HE and μCT image. A, μCT image (Bars: 200 μm): LELI group (L1–L5), non-irradiation group (N1–N5), HE (×100, Bars: 200 μm): LELI group (L6–L10), non-irradiation group (N6–N10), DBR, distobuccal root of first molar; MBR2, mesiobuccal root of second molar, Arrow FD, force direction, B, HE (×400, Bars: 50 μm): L6-a, L7-b, L8-c, L9-d, L10-e, N6-f, N7-g, N8-h, N9-I, N10-j; V, vessel; OC, osteoclast; OB, osteoblast; NB, new bone.

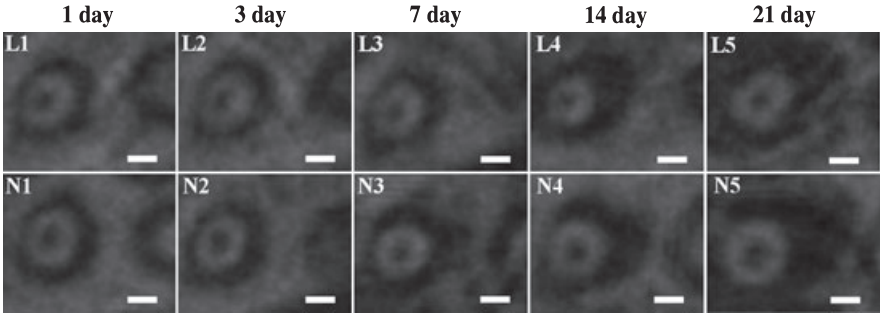

Fig. 9. Temporal μCT image (Bars: 200 μm). The periodontal ligament space was elongated in both groups with time. LELI group (L1–L5), non-irradiation group (N1–N5).

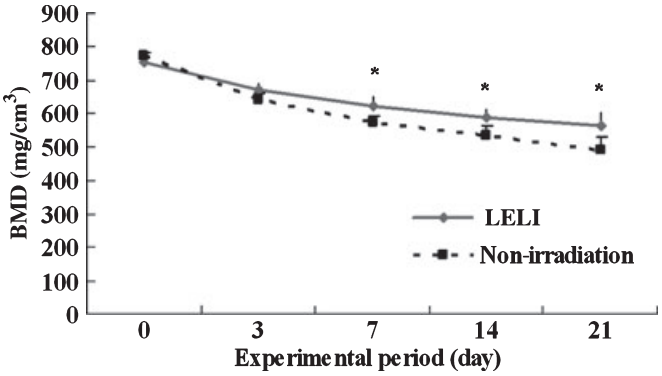

Fig. 10. BMD was significantly greater in the LELI group than in the non-irradiation group (*$p < 0.05$, N = 5).

the amount of tooth movement was significantly greater in the LELI group on day 7 (1.5-fold) than in the non-irradiation group, and Kawasaki et al. (7) showed that the amount of tooth movement was significant in the LELI group on day 12 (1.3-fold). In the present study, the amount of tooth movement was significantly greater in the LELI group on day 3 (1.4-fold), 7 (1.19-fold), 14 (1.26-fold), and 21 (1.34-fold) than in the non-irradiation group (Fig. 7). Luger et al. (26) reported that the scattering through the skin reduced the energy level of laser beams to 3–6% of its original intensity. Infrared laser irradiation had a low absorption coefficient in hemoglobin and water, and consequently, a high penetration depth in the irradiated tissue. It is well known that infrared radiation of 750 nm can penetrate more than visible radiation at 650 nm into soft tissues (27). As the objective of the present study was to stimulate bone cells which were placed deeply under the soft tissue (e.g., gingiva) in the PDL space, the infrared laser (810 nm) was selected for the present study. Therefore, the authors assumed that the energy of laser irradiation was delivered to the PDL through the mucosa/gingiva and alveolar bone in the present study.

Limpanichkul et al. (28) reported that LELI was too low to express either a stimulatory effect or inhibitory effect on the rate of orthodontic tooth movement. On the contrary, Youssef et al. (27) and Cruz et al. (29) demonstrated that LELI stimulated the velocity of tooth movement. With regard to the energy and wavelength of Ga–Al–As low-level laser apparatus, the total energy (75 J/cm^2) of laser used by Limpanichkul et al. was higher than that of Youssef et al. (8 J/cm^2) (27), Cruz et al. (50 J/cm^2) (29) and this study (54 J/cm^2). Furthermore, the wavelength of Limpanichkul et al. (860 nm) (28) was also longer than that of Youssef et al. (809 nm) (27), Cruz et al. (780 nm) (29) and this study (810 nm). Therefore, our irradiation conditions may be the optimal energy and wavelength of laser for stimulating the rate of orthodontic tooth movement. The above findings suggest that LELI increases the amount of tooth movement.

Then, BMD in the alveolar bone on the tension site was determined during LELI. The methods currently used for BMD measurement are dual energy X-ray absorptiometry (DXA) (30) using X-ray beams of two different energies, single energy X-ray absorptiometry (14) using an X-ray beam of one energy, peripheral quantitative computed tomography (pQCT) (31) using X-ray CT, and low-intensity pulsed ultrasound (32, 33) using an ultrasonic wave, etc. Although most reports of BMD in rat jaw-bone employed DXA (34, 35), Kuroda et al. (36) measured the BMD of rat mandible using a combination of pQCT and DXA. However, it is determined using the sample after sacrifice, and temporal change of the same sample cannot be determined. In the present study, we used R_mCT® that is a cone beam system, in which the X-ray arms rotate 360° focusing on a sample, resulting in scanning the whole of rat jaw-bone in only 17 s. These characteristics enabled reduction of exposure and the extent of anesthesia, and it is possible to scan the same sample temporally, since there is little harm to the experi-

mental animals (37–40). The CT images were taken *in vivo* and the pixel size of this CT is 30 μm. The absorption of X-rays by the bone was observed by the resolution of the CT image. We compared the CT image with the histopathological image that corresponded to the region of interest and the resolution of CT image. We performed this at low magnification for these reasons (Fig. 8A). The evaluation of the histopathological images themselves was performed under high magnification (Fig. 8B).

As a result of measurement, although both groups showed a temporal fall of BMD with the increase in amount of tooth movement, BMD was significantly greater in the LELI group on days 7 (1.08-fold), 14 (1.09-fold), and 21 (1.14-fold) as compared with the non-irradiation group (Fig. 10). Saito et al. (41) reported that LELI stimulated bone remodeling during rapid palatal expansion in rat MPS. Kawasaki et al. (7) also showed that LELI increased the bone formation on the tension side during experimental tooth movement in rat. Kim et al. (42) reported that LELI facilitated bone metabolism during bone healing in rats. Further, Hamajima et al. (43) reported that the increased expression of the osteoglycin gene by LELI in the early proliferation stage of cultured osteoblastic cells might play an important role in the stimulation of bone formation in combination with matrix proteins and growth factors. Moreover, Ozawa et al. (44) reported that LELI administered during the early stages of formation of osteoblast-like cells isolated from fetal rat calvariae significantly stimulated cellular proliferation, alkaline phosphatase (ALP) activity, and osteocalcin gene expression. Further, LELI in the earlier stages of cell cultures significantly stimulated the proliferation of osteoblasts, resulting in a greater number (1.7-fold) and larger area (3.4-fold) of bone nodules that developed in the culture dish on days 21. These results suggest that laser irradiation stimulates osteogenesis on the tension site, resulting in control of the decrease of BMD.

Several studies reported that osteoclasts appeared on the pressure site 17–20 h after force application during experimental tooth movement in rat (45–47), although only a few reports showed that osteoclasts were identified on the tension site (48). In the present study, HE findings demonstrated that in both groups osteoclasts appeared on the tension site on day 1 (Fig. 8A, L6, N6, B, L6-a and N6-f). These osteoclasts increased in number continuously till 3 days (Fig. 8A, L7, N7, B, L7-b and N7-g). Therefore, it is suggests that osteoclastogenesis is guided not only by the pressure force to the PDL and alveolar bone but also tension force. Moreover, there was a strong tendency for the increase in number of osteoclasts in the LELI group compared with the non-irradiation group until 3 days (Fig. 8A, L7, N7, B, L7-b and N7-g). Then, Fujita et al. (6) reported that LELI stimulated osteoclastogenesis on the pressure side; LELI may stimulate osteoclastogenesis not only on the pressure site but also on the tension site.

On the other hand, about the temporal reduction of BMD (Fig. 10), it could be due to the continuous application of orthodontic force for 22 days by NT-coil. In order to ensure periodontal tissue health, optimal tooth movement may be necessary with intermittent release of orthodontic force to allow time for tissue-recovery after moving a certain distance. Vignery et al. (49) reported that the remodeling cycle of rat alveolar bone rotated one time at the shortest in 6 days. In spite of considerable reduction of osteoclasts on day 7 (Fig. 8A, L8, N8) and trabecular bone formation on day 14 (Fig. 8A, L9, N9, B, L9-d and N9-i), the PDL had expanded further on day 21 and BMD decreased in both groups (Figs 8A, L5, N5, L10, N10, B, L10-e, N10-j and 10). These findings suggest that it may have been necessary to set a resting stage of orthodontic force for a certain fixed period of time between 14–21 days so that bone formation catches up with the amount of movement. In addition, it is the possible that occlusal trauma may have been produced because the occlusal condition varies with the increase in tooth movement (50).

Louridis et al. (51) reported that the thickness of normal PDL in rat was about 110–220 μm. In the present study, thickness of the PDL space after 1 day was not reduced throughout the experimental period as confirmed by the temporal μCT image of the same sample (Fig. 9, L1-5 and N1-5), and comparison with HE and μCT image (Fig. 8A, L1-10 and N1-10). This finding suggests the possibility that bone formation does not catch up with the amount of tooth movement. Not only the orthodontic force level but the optimal action period or the frequency of the load should be determined in further studies, and establishment of an experimental model that attains tooth movement quickly and more safely is needed.

Conclusion

LELI accelerates the velocity of tooth movement via stimulation of the alveolar bone remodeling during experimental tooth movement in rat.

Clinical relevance

In the field of orthodontics, LELI is utilized for several different types of clinical orthodontic treatment, such as reduction of post adjustment pain or treatment of traumatic ulcers in the oral mucosa promoted by an appliance. However, scant information is available concerning the effects of LELI on bone remodeling during orthodontic tooth movement. This might be a method to enhance tooth movement.

Acknowledgements: This research was supported in part by a Grant-in-Aid for Scientific Research from the Japan Society for the Promotion of Science (C:18592252, C: 19592367).

References

1. Sandstedt C. Einige Beitrage zur Theorie der Zahnregulierung. *Nord Tandilakere Tidssker* 1904;5:236–56.
2. Macapanpan LC. Early tissue changes following tooth movement in rats. *Angle Orthod* 1954;24:79–95.
3. Azuma M. Study on histologic changes of periodontal membrane incident to experimental tooth movement. *Bull Tokyo Med Dent Univ* 1970;17:149–78.
4. Eriksen EF, Axelrod DW, Melsen F. *Bone Histomorphometry*; in, 1st edn. New York: Raven press; 1994.
5. Yamaguchi M, Fujita S, Yoshida T, Okikawa K, Utsunomiya T, Yamamoto H et al. Low-energy laser irradiation stimulates the tooth movement velocity via expression of M-CSF and c-fms. *Orthod Waves* 2007;66:139–48.
6. Fujita S, Yamaguchi Y, Utsunomiya T, Yamamoto H, Kasai K. Low-energy laser irradiation stimulates tooth movement velocity via expression of RANK and RANKL. *Orthod Craniofac Res* 2008;11:143–55.
7. Kawasaki K, Shimizu N. Effects of low-energy laser irradiation on bone remodeling during experimental tooth movement in rats. *Lasers Surg Med* 2000;26:282–91.
8. Sennerby L, Thomsen P, Ericson LE. A morphometric and biomechanic comparison of titanium implants inserted in rabbit cortical and cancellous bone. *Int J Oral Maxillofac Implants* 1992;7:62–71.
9. Ericsson I, Johansson CB, Bystedt H, Norton MR. A histomorphometric evaluation of bone-to-implant contact on machine-prepared and roughened titanium dental implants. A pilot study in the dog. *Clin Oral Implants Res* 1994;5:202–6.
10. Evans GH, Mendez AJ, Caudill RF. Loaded and nonleaded titanium versus hydroxyapatite-coated threaded implants in the canine mandible. *Int J Oral Maxillofac Implants* 1996;11: 360–71.
11. Odgaard A, Gundersen HJ. Quantification of connectivity in cancellous bone, with special emphasis on 3-D reconstructions. *Bone* 1993;14:173–82.
12. Guilak F. Volume and surface area measurement of viable chondrocytes in situ using geometric modeling of serial confocal sections. *J Microsc* 1994;173:245–56.
13. Odgaard A. Three-dimensional methods for quantification of cancellous bone architecture. *Bone* 1997;20:315–28.
14. Hildebrand T, Ruegsegger P. Quantification of bone microarchitecture with the structure model index. *Comput Methods Biomech Biomed Engin* 1997;1:15–23.
15. Hildebrand T, Ruegsegger P. A new method for the model independent assessment of thickness in three-dimensional images. *J Microsc* 1997;185:67–75.
16. Uchiyama T, Tanizawa T, Muramatsu H, Endo N, Takahashi H, Hara T. A morphometric comparison of trabecular structure of human ilium between microcomputed tomography and conventional histomorphometry. *Calcif Tissue Int* 1997;61: 493–8.
17. Lang T, Augat P, Majumdar S, Ouyang X, Genant HK. Noninvasive assessment of bone density and structure using computed tomography and magnetic resonance. *Bone* 1998;22:149S–53S.
18. Muller R, van Campenhout H, van Damme B, van Der Perre G, Dequeker J, Hildebrand T et al. Morphometric analysis of human bone biopsies: a quantitative structural comparison of histological sections and micro-computed tomography. *Bone* 1998;23:59–66.
19. Beck TJ, Looker AC, Ruff CB, Sievanen H, Wahner HW. Structural trends in the aging femoral neck and proximal shaft: analysis of the third national health and nutrition examination survey dual-energy X-ray absorptiometry data. *J Bone Miner Res* 2000;15:2297–304.
20. Hara T, Takizawa M, Sato T, Ide Y. Mechanical properties of buccal compact bone of the mandibular ramus in human adults and children: relationship of the elastic modulus to the direction of the osteon and the porosity ratio. *Bull Tokyo Dent Coll* 1998;39:47–55.
21. Balto K, Muller R, Carrington DC, Dobeck J, Stashenko P. Quantification of periapical bone destruction in mice by micro-computed tomography. *J Dent Res* 2000;79:35–40.
22. Arai Y, Yamada A, Ninomiya T, Kato T, Masuda Y. Micro-computed tomography newly developed for in vivo small imaging. *Oral Radiol* 2005;21:14–8.
23. Yasko AW, Lane JM, Fellinger EJ, Rosen V, Wozney JM, Wang EA. The healing of segmental bone defects, induced by recombinant human bone morphogenetic protein (rhBMP-2). A radiographic, histological, and biomechanical study in rats. *J Bone Joint Surg Am* 1992;74:659–70.
24. Ren Y, Maltha JC, Kuijpers-Jagtman AM. The rat as a model for orthodontic tooth movement-a critical review and a proposed solution. *Eur J Orthod* 2004;26:483–90.
25. Kirino Y, Tsuchiya T, Kurihara S, Chiba M, Miura F. A study of tooth movement with super-elastic force. *J Jpn Orthod Soc* 1991;50:315–24.
26. Luger JE, Rochkind S, Wollman Y, Kogan G, Dekel S. Effect of low-power laser irradiation on the mechanical properties of bone fracture healing in rats. *Lasers Surg Med* 1998;22:97–102.

27. Youssef M, Ashkar S, Hamade E, Gutknecht N, Lampert F, Mir M. The effect of low-level therapy during orthodontic movement: a preliminary study. *Lasers Med Sci* 2008;23:27–33.
28. Limpanichkul W, Godfrey K, Srisuk N, Rattanayatikul C. Effects of low-level laser therapy on the rate of orthodontic tooth movement. *Orthod Craniofac Res* 2006;9:38–43.
29. Cruz DR, Kohata EK, Ribeiro MS, Wetter NU. Effects of low-intensity laser therapy on the orthodontic movement velocity of human teeth: a preliminary study. *Lasers Surg Med* 2004;35:117–20.
30. Ward KA, Cotton J, Adams JE. A technical and clinical evaluation of digital X-ray radiogrammetry. *Osteoporos Int* 2003;14:389–95.
31. Aranyarachkul P, Caruso J, Gantes B, Schulz E, Riggs M, Dus I et al. Bone density assessments of dental implant sites: 2. Quantitative cone-beam computerized tomography. *Int J Oral Maxillofac Implants* 2005;20:416–24.
32. Fini M, Giavaresi G, Setti S, Martini L, Torricelli P, Giardino R. Current trends in the enhancement of biomaterial osteointegration: biophysical stimulation. *Int J Artif Organs* 2004;27:681–90.
33. Iwabuchi S, Ito M, Hata J, Chikanishi T, Azuma Y, Hara H. In vitro evaluation of low-intensity pulsed ultrasound in herniated disc resorption. *Biomaterials* 2005;26:7104–14.
34. Mavropoulos A, Rizzoli R, Ammann P. Different responsiveness of alveolar and tibial bone to bone loss stimuli. *J Bone Miner Res* 2007;22:403–10.
35. Elsubeihi ES, Heersche JN. Quantitative assessment of post-extraction healing and alveolar ridge remodeling of the mandible in female rats. *Arch Oral Biol* 2004;49:401–12.
36. Kuroda S, Mukohyama H, Kondo H, Aoki K, Ohya K, Ohyama T. Bone mineral density of the mandible in ovariectomized rats: analyses using dual energy X-ray absorptiometry and peripheral quantitative computed tomography. *Oral Dis* 2003;9:24–8.
37. Arita K, Saito I, Arai Y. Evaluation of mouse gutter shaped root (s) as a quantitative trait using micro-CT. *Ped Dent J* 2006;16:23–7.
38. Osuga N, Yang J, Ninomiya T, Arai Y, Wang R, Iwasaki H et al. Micro-CT observation of rat dental pulp healing after pulpotomy in vivo study. *Ped Dent J* 2006;16:132–7.
39. Yang J, Osuga N, Wang R, Xu Q, Yanagisawa S, Nakade T et al. Observations of pulpotomy in rats using in vivo Micro-CT: the changes after treatment of formocresol and calcium hydroxide pulpotomies or CO_2 laser irradiation. *Ped Dent J* 2007;17:32–9.
40. Arai Y, Ninomiya T, Tanimoto H. Development of in vivo micro computed tomography using flat panel detector. *Dent Jpn (Tokyo)* 2007;43:109–11.
41. Saito S, Shimizu N. Stimulatory effects of low-power laser irradiation on bone regeneration in midpalatal suture during expansion in the rat. *Am J Orthod Dentofacial Orthop* 1997;111:525–32.
42. Kim YD, Song WW, Kim SS, Kim GC, Hwang DS, Shin SH et al. Expression of receptor of nuclear factor – kB ligand, receptor activator of nuclear factor – kB, and osteoprotegerin, following low-level laser treatment on deproteinized bovine bone graft in rats. *Lasers Med Sci* 2008, Sep 30, Epub ahead of print.
43. Hamajima S, Hiratsuka K, Kiyama-Kishikawa M, Tagawa M, Kawahara M, Ohta H et al. Expression of low-level laser irradiation on osteoglycin gene expression in osteoblasts. *Lasers Med Sci* 2003;18:78–82.
44. Ozawa Y, Shimizu N, Kariya G, Abiko Y. Low-energy laser irradiation stimulates bone nodule formation at early stages of cell culture in rat calvarial cells. *Bone* 1998;22:347–54.
45. Ouchi K. Studies on the changes of the alveolar bone during the experimental tooth movement, by means of labeling methods and microradiography. *Shigaku* 1974;61:1072–119.
46. Koga T. Histologic study on the periodontal structures incident to experimental tooth movement in rats – light-microscopic and electron-microscopic investigations. *Shikwa Gakuho* 1974;74:498–557.
47. Kurihara S. An electron microscopic observation on cells found in bone resorption area incident to experimental tooth movement. *Bull Tokyo Med Dent Univ* 1977;24:103–23.
48. Shiohama Y. Histological and immunocytochemical study of bone resorption and endothelin-1 localization in experimental tooth movement. *Orthod Waves* 1994;53:457–71.
49. Vignery A, Baron R. Dynamic histomorphometry of alveolar bone remodeling in adult rat. *Anat Rec* 1980;196:191–200.
50. Yagishita H, Sato K, Warita S, Ando F, Aoba T. Enzyme- and immuno-histochemical studies on root resorption activities accompanied by the physiological and orthodontic tooth movement of rat molars. *Jpn J Oral Biol* 2000;42:283–92.
51. Louridis O, Demetriou N, Bazopoulou KE. Periodontal ligament thickness as related to age and mesiocclusal drifting of teeth: a histometric study. *J Periodont* 1974;45:862–5.